



Conduction band modifications by d states in vanadium doped CdO

Y.J. Li ^{a, b}, K.M. Yu ^{c, d, *}, G.B. Chen ^e, Chao Ping Liu ^{c, f}, W. Walukiewicz ^{a, g, **}^a Materials Sciences Division, Lawrence Berkeley National Laboratory, Berkeley, CA, 94720, USA^b Electronic Science Department, Huizhou University, Huizhou, 516007, China^c Department of Physics, City University of Hong Kong, Kowloon, Hong Kong^d Department of Materials Science and Engineering, City University of Hong Kong, Kowloon, Hong Kong^e Physics Department and Jiangsu Key Laboratory for Chemistry of Low Dimensional Materials, Huaiyin Normal University Jiangsu, China^f Department of Physics, College of Science, Shantou University, Shantou, Guangdong, 15063, China^g Department of Materials Science and Engineering, University of California, Berkeley, CA, USA

ARTICLE INFO

Article history:

Received 6 September 2019

Received in revised form

25 December 2019

Accepted 26 December 2019

Available online 27 December 2019

Keywords:

Band anticrossing

Cadmium oxide

Optical absorption

Effective mass

Transparent conductor

ABSTRACT

3d transition metal ions have been shown to act as donors and to introduce highly localized d-levels when incorporated in CdO. In this work, we synthesized CdO thin films doped with a 3d metal V (CVO) with a V mole fraction x up to 0.1 by radio-frequency magnetron sputtering. CVO thin films exhibit a monotonic increase in the electron concentration n with x up to a saturation value of $\sim 1.0 \times 10^{21} \text{ cm}^{-3}$ at a dopant concentration $x > 0.045$. In contrast to CdO doped with shallow donors such as In where the electron mobility μ is $> 100 \text{ cm}^2/\text{V-s}$ even at a high In doping level of $> 5\%$, in CVO the μ decreases continuously from ~ 100 to $< 10 \text{ cm}^2/\text{V-s}$ with increasing x . Spectroscopic ellipsometry measurements show a rapid increase in the effective mass in CVO, consistent with the continuous reduction of μ . The electrical and optical properties of CVO are analyzed in terms of the anticrossing interaction of the localized V d-levels with the extended conduction band (CB) states of the host CdO. Such anticrossing interaction splits the CdO CB into two non-parabolic subbands, E_+ and E_- . The optical absorption edge of CVO with $x > 0.045$ is consistent with transitions from the valence band to the empty E_+ subband while the much reduced μ can be explained by the increase in effective mass due to flattening of the E_- subband. Such band anticrossing interaction is a common phenomenon for most transition metal dopants with d electrons in metal oxides and can explain the optoelectronic properties of these materials.

© 2020 Elsevier B.V. All rights reserved.

1. Introduction

Transparent conducting oxides (TCOs) are wide gap simple metal oxides with high conductivity and transparency in the visible spectral range, which have been widely used in thin film solar cells, displays, and other optoelectronic devices [1–5]. Cadmium oxide (CdO) was the first TCO discovered in 1907 [6] but has not found wide application because of its relatively small direct band gap of 2.2 eV. Recently, CdO has found renewed interests due to its unusual electronic band structure [7–9]. Intentionally doped CdO with electron concentration exceeding $10^{21}/\text{cm}^3$ and with electron

mobility larger than $100 \text{ cm}^2/\text{V-sec}$ has been achieved [10–14]. This high electron concentration gives rise to a pronounced Burstein-Moss (BM) shift extending the absorption edge to $> 3 \text{ eV}$ [11,14–16]. High conductivity ($> 10^4 \text{ S cm}^{-1}$) and excellent transmission covering a spectral range of 400 to $> 1500 \text{ nm}$ have been reported for appropriately doped CdO samples, making it an ideal TCO for full spectrum photovoltaics [11,13].

Investigations aimed at tailoring the electrical and optical properties of CdO have focused primarily on conventional hydrogenic dopants such as Ga, In and Sn [10–12,14,15,17]. All of these dopants are shallow donors in CdO with similar core electron shells configuration with Cd atom. Transition metal (TM) ions such as Y and Sc, with partially filled outer d-shells have also been studied as n-type dopants into CdO [12,18,19]. Although these TM ions may contribute free electrons and act as effective donors in CdO, their unfilled d-shells formed localized states and interact with the original band structure of the semiconductor host, which may result in unexpected electrical and optical properties. Vanadium (V)

* Corresponding author. Department of Physics, City University of Hong Kong, Kowloon, Hong Kong.

** Corresponding author. Materials Sciences Division, Lawrence Berkeley National Laboratory, Berkeley, CA, 94720, USA.

E-mail addresses: kinmanyu@cityu.edu.hk (K.M. Yu), w_walukiewicz@lbl.gov (W. Walukiewicz).

belongs to the 3d transition metal group with $3d^24s^2$ valence electron shell. Substitution of V atom on Cd site introduces highly localized d-levels in CdO. We also note that doping of other TCOs with TMs has been reported. In particular, previous studies have shown that doping of In_2O_3 with a 4d transition metal Mo produces high electron mobility n-type material. For most of these cases, the electron concentration was on the order of $1\text{--}3 \times 10^{20}/\text{cm}^3$, suggesting that the Mo doping concentration is only on the order of $\sim 1\%$. The effect has been attributed to doping by transfer of electrons from 4d charge transition states located high above the conduction band edge of In_2O_3 [20–23].

The energies of the localized d-donor and d-acceptor states in II-VI compounds were compiled by Langer et al. [24]. It was shown that because of their localized nature, the d shell derived states remain constant on the absolute scale relative to the vacuum level. This allows prediction of the energy of the d states from the known band offset between different II-VI semiconductors. V ions substituting cations in II-VI semiconductors form a localized d-donor level about 5 eV below the vacuum level [25]. Since the electron affinity of CdO was previously determined to be ~ 5.8 eV [8,26,27], the V localized d donor levels will be located at ~ 0.8 eV above the conduction band (CB) minimum of CdO. When an V substitutes a Cd, the 2 4s electrons participate in chemical bonds by replacing 2 5s electrons of Cd. Because of the very low location of the CdO conduction band edge, one of the V 3d electrons drops to the conduction band and hence provides a free electron for conduction. Moreover, at high V doping the CB of the material will be modified through the interaction of these localized d states with the extended CB states of CdO, similar to the band anticrossing interaction in highly mismatched alloys [28–31]. In this work, we explore the electronic band structure modifications of CdO by the d states of the V dopant and their effects on the electrical and optical properties of this material.

2. Experimental

V-doped and In-doped CdO were deposited by RF magnetron sputtering method on glass substrates. Two separate sputtering targets, CdO and V_2O_3 for $\text{Cd}_{1-x}\text{V}_x\text{O}$, and CdO and In_2O_3 for $\text{Cd}_{1-y}\text{In}_y\text{O}$ were used. The composition was controlled by varying the sputtering power and target to substrate distance of the individual target. All the films were deposited at a substrate temperature between 170°C and 270°C with film thicknesses in the range of 140350 nm. Prior to deposition, the chamber was pumped down to $<1 \times 10^{-6}$ Torr. During the deposition, the background pressure was maintained at 5 mTorr by flowing Ar.

The crystalline structure of as-grown films was determined by x-ray diffraction (XRD) using a Siemens D500 diffractometer. The film composition and thickness were characterized by Rutherford backscattering spectrometry (RBS) with 3.04 MeV He^{++} ion beam. The electron concentration and carrier mobility were measured by Hall Effect in the Van der Pauw configuration using an Ecopia HMS-3000 system with a 0.6 T magnetic field. Transmittance and reflectance measurements were carried out using a PerkinElmer Lambda 950 spectrophotometer with a Universal Reflectance Accessory. Variable angle spectroscopic ellipsometry (VASE) measurements in the spectral range of 190–1700 nm (0.73–6.5 eV) were carried out using a rotating-compensator instrument (J. A. Woollam, M – 2000) to study the optical properties of the samples. Details of the VASE measurements and analysis were published in Ref. [15].

3. Results and discussion

Fig. 1(a) shows the XRD scans of CVO ($x = 0.002\text{--}0.09$) in the 2θ

range of $30^\circ \sim 70^\circ$. The standard diffraction pattern for CdO (PDF 05–0640) is also shown for comparison. All of the as-grown films show a rocksalt structure with no observable secondary phase present. With increasing V content in the film, grains change from (111) to (200) preferred orientation. High resolution scans in the 2θ range of $32^\circ \sim 39^\circ$ shown in Fig. 1(b) reveal that the diffraction peaks gradually shift to higher diffraction angles with increasing V fraction, suggesting that the lattice parameter decreases with increasing V content. This is consistent with the substitution of Cd (with an ionic radius of 0.95 Å) with V ions which have a smaller ionic radius of 0.79 Å. The inset of Fig. 1(b) shows $[\text{CdO}_6]$ octahedra organized in a rocksalt lattice with NaCl structure type.

Fig. 2 shows the electrical properties of V and In doped CdO films. The electron concentration in CVO monotonically increases from $2.2 \times 10^{20} \text{ cm}^{-3}$ to $1.0 \times 10^{21} \text{ cm}^{-3}$ with increasing x from 0 to 0.048, then saturates at $\sim 1.0 \times 10^{21} \text{ cm}^{-3}$ when $x \geq 0.048$. This suggests that V is an effective donor in CdO up to a doping level of $\sim 5\%$. In contrast, for In-doped CdO, the electron concentration shows a continuous increase, even for In doping as high as 10%. Fig. 2 also shows that the composition dependence of the mobility μ in V and In doped CdO differs drastically. For In-doped CdO, the mobility increases from $104 \text{ cm}^2/\text{V-s}$ in undoped CdO to $120 \text{ cm}^2/\text{V-s}$ ($y < 2.7\%$) and then gradually decreases to a stable value of $\sim 80 \text{ cm}^2/\text{V-s}$ for In content as high as $y \sim 0.10$. Similar high mobility CdO thin films doped heavily with Sn [10] and Ga [11,14] have also been reported previously. In comparison, the mobility in CVO rapidly decreases from 104 to $8 \text{ cm}^2/\text{V-s}$ as the V content increases. Similar decrease in the mobility with dopant concentration has been reported for other TM dopants in CdO, such as Y [12,19] and Sc [12]. This is not surprising as both Y and Sc also have unfilled d-orbits and are expected to introduce highly localized donor states in CdO. Yang et al. performed First-principles electronic band structure calculations and suggested that the presence of the “d states” of Y and Sc affects the dispersion and reduces the electron mobility [12].

Optical properties of the films were measured by variable angle spectroscopic ellipsometry (VASE). VASE data were analyzed using the Drude model combined with the Tauc-Lorentz model to obtain the dielectric function of CdO films doped with V as well as In and Ga shallow dopants [16,32]. The effective mass was extracted from the expression for the plasma energy E_p ,

$$E_p = \sqrt{\frac{\hbar^2 e^2 N_{\text{opt}}}{m^* \epsilon_\infty \epsilon_0}}, \quad (1)$$

where N_{opt} , ϵ_∞ and ϵ_0 are the optical carrier concentration, high frequency dielectric constant and permittivity of free space, respectively. Here, E_p and ϵ_∞ are obtained from fitting the VASE data, while N_{opt} is taken as the carrier concentration measured by Hall effect, n [16]. Fig. 3 shows the effective mass as a function of n for CdO thin films doped with In, Ga and V. The effective mass for the Ga and In doped CdO show a monotonic sublinear increase with the electron concentration while that for CVO shows a rapid increase at $n > 8 \times 10^{20} \text{ cm}^{-3}$, corresponding to samples with a V content $x > 0.04$. According to Refs. [33,34] the concentration dependence of the effective mass can be given by,

$$m^* = m_0^* \sqrt{1 + 2C \frac{\hbar^2}{m_0^*} (3\pi^2 N)^{\frac{2}{3}}}. \quad (2)$$

where C is a parameter related to the nonparabolicity of the conduction band of CdO. The dashed line in Fig. 3 shows a fit of Eq. (2) to the In and Ga doped CdO effective mass data. The best fit was achieved with the effective mass at the bottom of the conduction band $m_0^* = 0.13m_0$ and a nonparabolicity parameter $C = 0.49 \text{ eV}^{-1}$

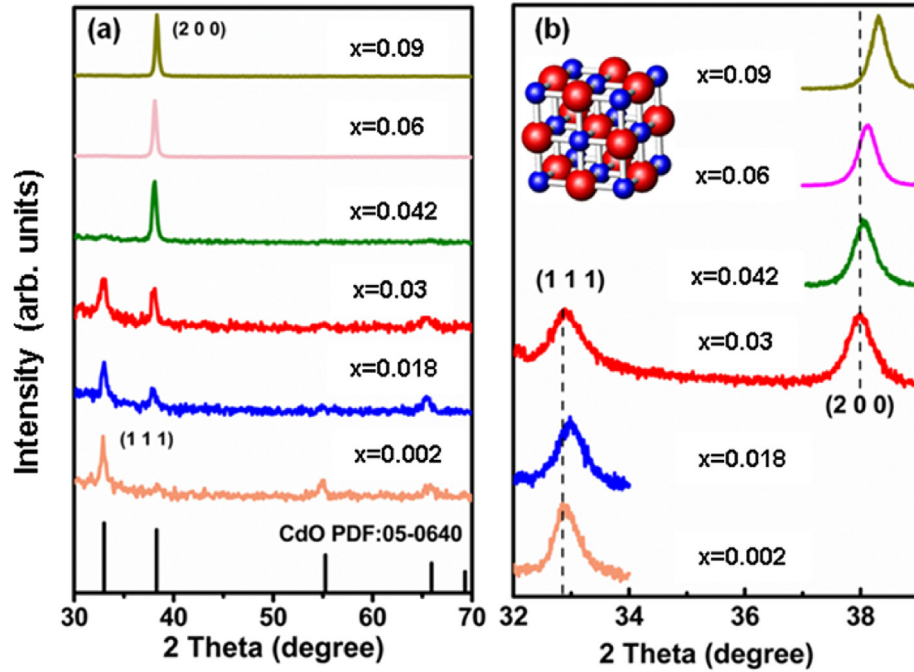


Fig. 1. (a) XRD patterns from $\text{Cd}_{1-x}\text{V}_x\text{O}$ films with $x = 0.002$ – 0.09 . (b) Detailed scans with 2θ range of 32° to 39° . The inset shows the crystal structure of CdO.

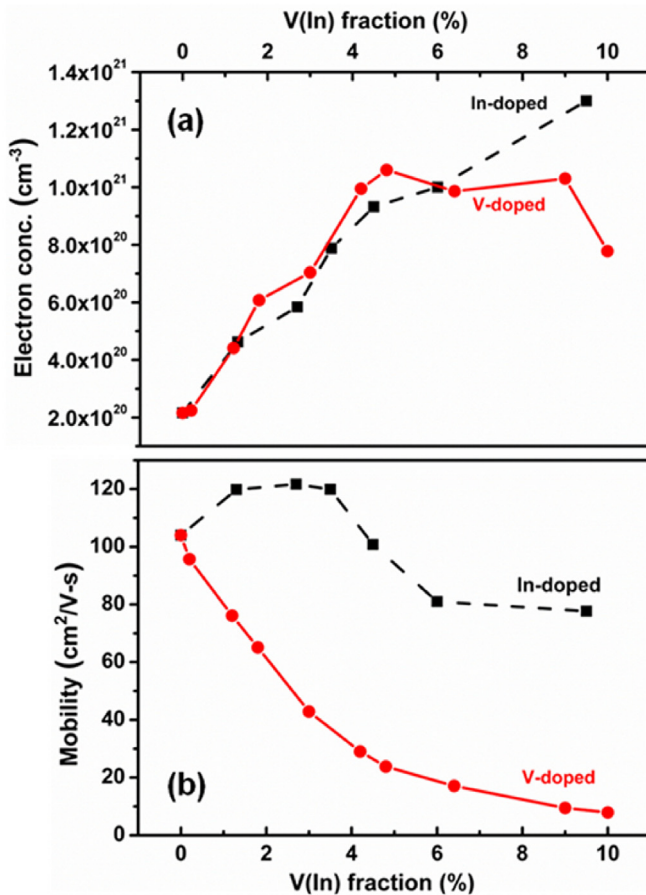


Fig. 2. (a) Electron concentration n and (b) mobility μ of V-doped and In-doped CdO as a function of dopant (In or V) concentration.

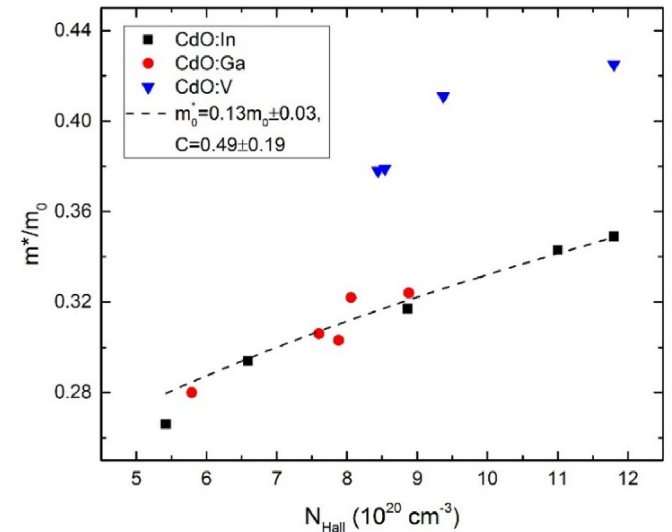


Fig. 3. Electron effective mass m^* for $\text{Cd}_{1-x}\text{V}_x\text{O}$ thin films as compared to that doped with In and Ga. The black line is the best fit for data from the In and Ga doped samples by using Eq. (2).

[16]. The abrupt increase of the effective mass of CVO is consistent with the low mobility observed in these samples (Fig. 2) but cannot be explained simply by the conduction band nonparabolicity.

In order to understand the origin of this unusual concentration dependence of the effective mass in CVO we note that introduction of localized states close to the conduction (or valence) band edge of a semiconductor leads to an anticrossing interaction between these localized states and the extended band states. The interaction described by the band anticrossing model (BAC) [28–31] strongly modifies dispersion relations of the host conduction (or valence band). A prominent example of a material with BAC interaction is $\text{GaN}_x\text{As}_{1-x}$ alloy where the anticrossing interaction of localized N

states with the CB states of GaAs splits the GaAs CB into a higher (E_+) and a lower (E_-) subbands. The energies of the subbands can be expressed as

$$E_{\pm}(k) = \frac{1}{2} \left\{ \left[E_k^c + E^d \right] \pm \sqrt{\left[E_k^c - E^d \right]^2 + 4c^2x} \right\}, \quad (3)$$

where E_k^c is the unperturbed energy dispersion of the lowest CB of the host semiconductor, E^d is the energy of the localized states derived from the substitutional N atoms, c is the hybridization parameter describing the coupling between the localized states and the band states of the host, and x is the dopant concentration [28]. The extremely low location of the CB edge of CdO at around 5.8 eV below the vacuum level E_{vac} places the donor d -state of V ($d(3/2)$) at $E_d \sim 0.8$ eV above the CdO CB edge [8,25,26]. However, in contrast to the case of isovalent N in GaAs, V also acts as a donor in CVO and therefore free electron effects on the electronic band structure of CdO have to be taken into account. Garcia-Hemme et al. investigated the optical and electrical properties of V doped ZnO and showed that the band anticrossing of localized V $3d$ levels with extended states of the ZnO conduction band resulted in an upward shift of the mostly unoccupied conduction band states (E_+ sub-band) and a downward shift of an occupied narrow band derived from V donor d -levels (E_- sub-band) [35]. Francis et al. explained the positive band gap bowing and the variation of electrical properties of $\text{Cd}_{1-x}\text{Ni}_x\text{O}$ alloys with x over the entire composition range by the band anticrossing of Ni d states and the CdO CB [36]. However, in both previous cases the concentrations of electrons was limited and did not allow for detail studies of the effects of BAC on the electrical properties of the alloys. In the case of CVO the substitutional V atoms introduce localized states deep in the conduction band that act as donors contributing electrons to the conduction band.

To better understand the effects of the band anticrossing in V doped CdO, we investigated the optical properties of CVO. Fig. 4(a) shows the absorption coefficient α of CVO thin films with x ranging from 0 to 0.09 obtained from transmission and reflection measurements. In order to accurately obtain the absorption edge, instead of using the common α^2 extrapolation method, we fit the absorption coefficient curves shown in Fig. 4(a) using the expression [37]:

$$\alpha(E) = \frac{1}{\Delta\sqrt{\pi}} \int_{-\infty}^{\infty} \alpha_0(E' - E_g)^{1/2} \times \left[1 + \exp\left(\frac{E_F^* - E'}{kT}\right) \right]^{-1} \times \exp \left[-\left(\frac{E' - E}{\Delta}\right)^2 \right] dE', \quad (4)$$

where Δ is the Gaussian broadening parameter, α_0 is the ideal absorption coefficient of CdO, E_g is the intrinsic band gap of CdO, and E_F^* represents the optical band gap including Burstein-Moss (BM) shift. The best fits of the data using Eq. (4) are plotted in Fig. 4(a) as black solid lines. Note that α_0 is set to $2.3 \times 10^5 \text{ cm}^{-1}$ while Δ and E_F^* are fitting parameters. The fittings give the Δ values in the range between 0.35 and 0.42 eV. The optical band gap E_F^* of CVO obtained from the fittings are plotted in Fig. 4(b) as green triangles, while those of $\text{Cd}_{1-y}\text{In}_y\text{O}$ series are also shown as red circles for comparison.

We note that in Fig. 4(b) the absorption edge of $\text{Cd}_{1-y}\text{In}_y\text{O}$ increases with n as expected from free carrier effects, namely the Burstein-Moss (BM) shift and band renormalization [2,11,12,14–17,38]. This is consistent with the monotonic increase in electron concentration with In concentration up to $y \sim 0.1$. Similar large shifts of the absorption edge to higher energy for CVO with increasing V concentration x are also observed. However, Fig. 2(a) shows that for CVO after an initial increase in n with x (for $x < 0.04$), n saturates at $\sim 1.0 \times 10^{21} \text{ cm}^{-3}$ for $x > 0.04$ and even slightly drops for higher x . Nevertheless, the absorption edge does not reflect such saturation but continues shifting toward higher energy for $x > 0.04$ (open triangles in Fig. 4(b)). This suggests that the modification of the electronic band structure due to V d -levels also plays a significant role in the absorption properties in CVO.

We believe that similar to the case of V doped ZnO [35], the unusual optical absorption for CVO samples with V doping higher than $x \sim 0.04$ comes from the transitions between the valence band and the empty E_+ band. Fig. 5(a) shows the absorption edge energy for CVO shown in Fig. 4(b) plotted as a function of V content x . A good fit of the optical edge for samples with $x > 0.04$ is obtained using Eq. (3) for E_+ with $c = 2.3$ eV and $E^d = E_{VB} + 3.07$ eV (solid line) corresponding to $E^d \sim 4.93$ eV below E_{vac} . This E^d value is in a reasonable agreement with $E^d = 3.3$ eV estimated using V levels in

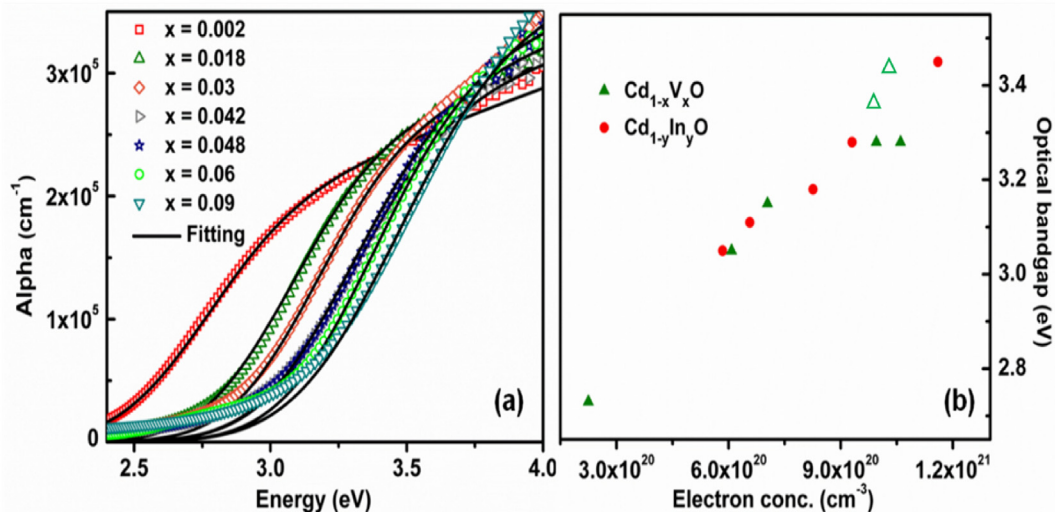


Fig. 4. (a) Absorption coefficient of $\text{Cd}_{1-x}\text{V}_x\text{O}$ ($x = 0.002$ – 0.09). The black lines in the figure indicate the best fit using equation (4). (b) Optical bandgaps as a functions of electron concentration in $\text{Cd}_{1-x}\text{V}_x\text{O}$ and $\text{Cd}_{1-y}\text{In}_y\text{O}$.

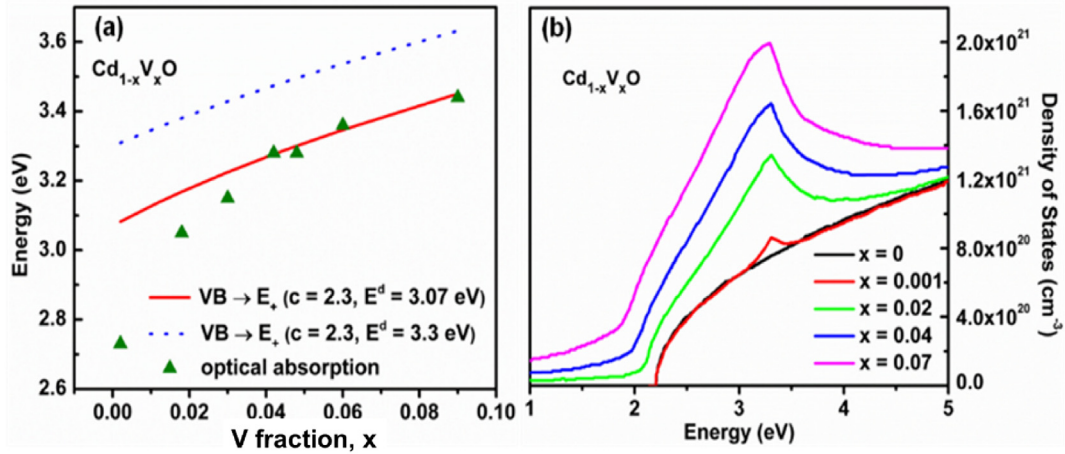


Fig. 5. (a) Absorption edge of $\text{Cd}_{1-x}\text{V}_x\text{O}$ as a function of V content x . The solid line shows the best fit using Eq. (1) with $c = 2.3$ eV and $E_d = 3.07$ eV. The dotted line shows the same fit with $E_d = 3.3$ eV. (b) DOS of the E_+ band of $\text{Cd}_{1-x}\text{V}_x\text{O}$ calculated using the parameters obtained from the best fit in (a).

II-VI from Langer et al. [24] and known band offset between different II-VI semiconductors. Previously we have determined the location of the conduction band edge (CBE) of ZnO at -4.9 eV below E_{vac} using a combination of soft x-ray absorption and emission spectroscopy and energetic ion irradiation [39]. Optical characterization of $\text{Zn}_{1-x}\text{V}_x\text{O}$ alloys by Garcia-Hemme suggested that the V d-level is located at ~ 0.13 eV below the CBE of ZnO [35], or ~ 5.03 eV below E_{vac} . This is in excellent agreement with our determination of the E^d level energy. Fig. 5(b) shows the calculated V doping dependent CB density-of-state (DOS) using our c and E^d parameters. Compared with undoped CdO, the DOS near the localized d-level exhibits significant increase with increasing V fraction, indicating more available states in the range of 2.5–4 eV introduced by V doping.

Fig. 6(a) shows the calculated dispersion relations for CVO with $x = 0.048$. The two non-parabolic bands E_+ and E_- appear due to the BAC effect where the E_+ -subband with more localized character and the E_- -subband with more extended-like character. Furthermore, Fig. 6(b) presents the dependence of E_+ and E_- edges on the V fraction. Fermi level energies of the CVO films with different V fraction as calculated from the measured electron concentration

are also shown as red circle symbols. The blue dashed line is drawn for the E_F data to guide the eye. A gradual up-shift from 3.07 eV to 3.45 eV for E_+ and down-shift from 2.20 eV to 1.82 eV for E_- with respect to the VB are observed with increasing V fraction from 0 to 9%. For those samples with saturated electron concentration ($x > 0.04$), the optical transitions mainly happen from the top of VB to the bottom of E_+ band, giving rise to the continuous increase of the absorption edge.

Since the dispersion of the E_- subband is significantly modified due to the BAC of the V d level and CdO CB states, as shown in Fig. 6(a), we expect that the electron effective mass in E_- (m_-^*) to be very different than those in the CdO CB (m_c^*). We estimate the m_-^* from the dispersion relation for the E_- subband using the standard expression,

$$m_-^* \approx \hbar^2 \left. \frac{k}{dE_-/dk} \right|_{k=\sqrt{3\pi^2 n}} \quad (5)$$

where $E_-(k)$ is given by Eq. (3) for alloys with different x , dE_-/dk represents the slope of the E_- dispersion, n is the electron concentration given in Fig. 2. Fig. 7 shows the measured mobility μ and

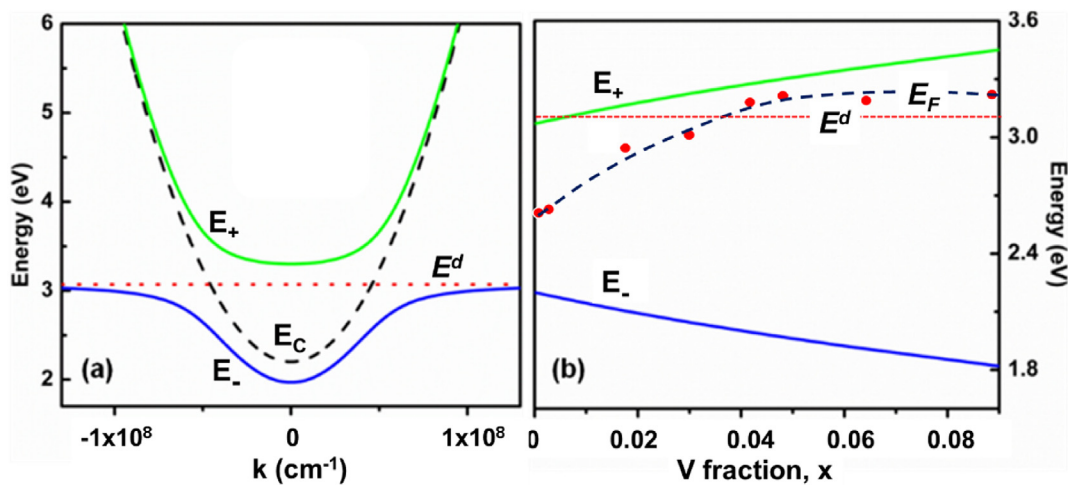


Fig. 6. (a) Dispersion relations of the restructured CB of $\text{Cd}_{1-x}\text{V}_x\text{O}$ with $x = 0.048$. (b) Dependence of E_+ and E_- transitions on V fraction. All of the energies are referenced to the top of the VB of CdO. Fermi level energies of the CVO films with different V fraction as calculated from the measured electron concentration are also shown as red circle symbols. (For interpretation of the references to colour in this figure legend, the reader is referred to the Web version of this article.)

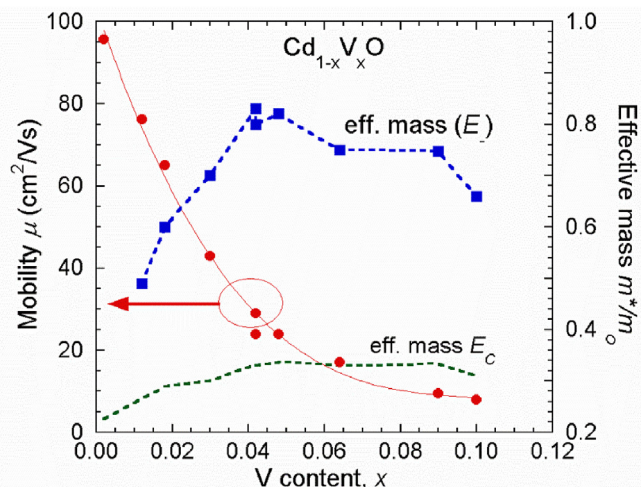


Fig. 7. Electron mobility μ measured by Hall effect and the calculated m^* as well as m_C^* for $\text{Cd}_{1-x}\text{V}_x\text{O}$ with x from 0 to 0.1.

the calculated m^* for CVO with x from 0 to 0.1. Also shown in Fig. 7 is the electron concentration dependent m_C^* calculated by Eq. (2) for the conduction band without BAC interaction. It is seen that values of m^* are almost 3 times larger m_C^* . This is a reflection of the much flatter dispersion of the E_- subband compared with unperturbed conduction band of CdO. Since $\mu = \frac{q}{m^*} \tau$, where q is the electron charge and τ is the mean free time, the rapid decrease in μ with x is consistent with the large increase of the effective mass of the E_- subband. Although the effective masses for CVO measured by SE shown in Fig. 3 are much larger than those for $\text{Cd}_{1-y}\text{In}_y\text{O}$ (m_C^*), they are ~ 2 times smaller than the calculated m^* . We note that the dispersion calculated by Eq. (3) is an estimate, especially for values far away from $k = 0$. Moreover, another source of error may be the assumption that N_{opt} is the same as the carrier concentration measured by Hall effect in Eq. (1). Nevertheless, our experimental μ and m^* are in qualitative agreement with those calculated from the BAC model.

4. Conclusions

$\text{Cd}_{1-x}\text{V}_x\text{O}$ and $\text{Cd}_{1-y}\text{In}_y\text{O}$ films were deposited by RF magnetron sputtering with dopant concentration up to 10%. While a continuous increase in electron concentration with high electron mobility of $>80 \text{ cm}^2/\text{V}$ were observed for In doping, V doped CdO shows a saturation in the electron concentration at $\sim 1.0 \times 10^{21} \text{ cm}^{-3}$ for $x \sim 0.04$ with a continuous drop in mobility to $<10 \text{ cm}^2/\text{V}$. The continuous increase in the absorption edge with V doping even beyond the saturated electron concentration level cannot be explained by free carrier effects as in In doped CdO. The electrical and optical properties of $\text{Cd}_{1-x}\text{V}_x\text{O}$ were analyzed in terms of the anticrossing interaction of the localized V d-levels with the extended conduction band (CB) states of the host CdO, splitting the CdO CB into two non-parabolic subbands E_+ and E_- . The optical absorption edge of $\text{Cd}_{1-x}\text{V}_x\text{O}$ with $x > 0.04$ is consistent with transitions from the valence band to the empty E_+ subband while the much reduced μ can be explained by the increase in effective mass due to flattening of the E_- subband. We expect that such band anticrossing interaction can be generalized for most transition metal dopants with d electrons in metal oxides and can explain the optoelectronic properties of these materials.

Declaration of competing interest

The authors declare that they have no known competing financial interests or personal relationships that could have appeared to influence the work reported in this paper.

CRediT authorship contribution statement

K.M. Yu: Formal analysis, Writing - review & editing, Supervision. **G.B. Chen:** Resources. **Chao Ping Liu:** Data curation. **W. Walukiewicz:** Methodology, Writing - review & editing, Supervision.

Acknowledgements

The work performed at LBNL was supported by the Director, Office of Science, Office of Basic Energy Sciences, Materials Sciences and Engineering Division, of the U.S. Department of Energy under Contract No. DE-AC02-05CH11231. This work was supported by the General Research Fund of the Research Grants Council of Hong Kong SAR, China, under Project No. CityU 11267516 and CityU SGP 9380076. YJL acknowledges the support of the National Natural Science Foundation of China under Project No. 51602121 and the Program for Innovative Research Team of Huizhou University (IRTHZU). YJL was also supported by China Scholarship Council.

References

- [1] D.S. Ginley, H. Hosono, D.C. Paine, *Handbook of Transparent Conductor*, Springer, New York, 2010.
- [2] P.D.C. King, T.D. Veal, J. Phys.: Condens. Matter 23 (2011) 334214.
- [3] K. Ellmer, Past achievements and future challenges in the development of optically transparent electrodes, *Nat. Photonics* 6 (2012) 809.
- [4] K.L. Chopra, P.D. Paulson, V. Dutta, *Prog. Photovolt. Res. Appl.* 12 (2004) 69.
- [5] Monica Morales-Masis, Rachel Stefaan De Wolf, Joel W. Ager Woods-Robinson, Christophe Ballif, *Adv. Electron. Mater.* (2017) 1600529.
- [6] K. Badeker, *Ann. Phys.* 22 (1907) 749.
- [7] L.F.J. Piper, Alex DeMasi, Kevin E. Smith, A. Schleife, F. Fuchs, F. Bechstedt, J. Zuniga-Perez, V. Munoz-Sanjose, *Phys. Rev. B* 77 (2008) 125204.
- [8] D.T. Speaks, M.A. Mayer, K.M. Yu, S.S. Mao, E.E. Haller, W. Walukiewicz, *J. Appl. Phys.* 107 (2010) 113706.
- [9] M. Burbano, D.O. Scanlon, G.W. Watson, *J. Am. Chem. Soc.* 38 (2011) 15065.
- [10] M. Yan, M. Lane, C.R. Kannewurf, R.P.H. Chang, *Appl. Phys. Lett.* 78 (2001) 2342.
- [11] K.M. Yu, M.A. Mayer, D.T. Speaks, H. He, R. Zhao, L. Hsu, S.S. Mao, E.E. Haller, W. Walukiewicz, *J. Appl. Phys.* 111 (2012) 123505.
- [12] Y. Yang, S. Jin, J.E. Medvedeva, J.R. Ireland, A.W. Metz, J. Ni, M.C. Hersam, A.J. Freeman, T.J. Marks, *J. Am. Chem. Soc.* 127 (2005) 8796.
- [13] E. Sachet, C.T. Shelton, J.S. Harris, B.E. Gaddy, D.L. Irving, S. Curtarolo, B.F. Donovan, P.E. Hopkins, P.A. Sharma, A.L. Sharma, J. Ihlefeld, S. Franzen, J.P. Maria, *Nat. Mater.* 14 (2015) 414.
- [14] D. M. Detert Kin Man Yu, Guibin Chen, Wei Zhu, Chaoping Liu, S. Grankowska, L. Hsu, O.D. Dubon, Wlodek Walukiewicz, *J. Appl. Phys.* 119 (2016) 18150.
- [15] A. Segura, J.F. Sanchez-Royo, B. Garia-Domene, G. Almonacid, *Appl. Phys. Lett.* 99 (2011) 151907.
- [16] Chao Ping Liu, Yishu Foo, M. Kamruzzaman, Chun Yuen Ho, J.A. Zapien, Wei Zhu, Y.J. Li, Wlodek Walukiewicz, Kin Man Yu, *Phys. Rev. Appl.* 6 (2016), 064018.
- [17] Yuankun Zhu, Rueben J. Mendelsberg, Jiaqi Zhu, Jiecai Han, Andre Anders, *Appl. Surf. Sci.* 265 (2013) 738.
- [18] Shu Jin, Yu Yang, Julia E. Medvedeva, John R. Ireland, Andrew W. Metz, Ni Jun, Carl R. Kannewurf, J. Arthur, Freeman, Tobin J. Marks, *J. Am. Chem. Soc.* 126 (2004) 13787.
- [19] Mengting Xie, Wei Zhu, Man Yu Kin, Zishu Zhu, Guanzhong Wang, *J. Alloy. Comp.* 776 (2019) 259.
- [20] C. Warmisnigh, Y. Yoshida, D.W. Readey, C.W. Teplin, J.D. Perkins, P.A. Parilla, L.M. Gedvilas, B.M. Keyes, D.S. Ginley, *J. Appl. Phys.* 95 (2004) 3831.
- [21] Naomii Yamada, Masayoshi Yamada, Haruna Toyama, Ryuichiro Ino, Xiang Cao, Yuuki Yamaguchi, Yoshihiko Ninomiya, *Thin Solid Films* 626 (2017) 46–54.
- [22] Jian Xu, Jian-Bo Liu, Bai-Xin Liu, Shun-Ning Li, Su-Huai Wei, Bing Huang, *Adv. Electron. Mater.* 4 (2018) 1700553.
- [23] Jack E.N. Swallow, Benjamin A.D. Williamson, Sanjayan Sathasivam, Max Birkett, Thomas J. Featherstone, Philip A.E. Murgatroyd, Holly J. Edwards, Zachary W. Lebens-Higgins, David A. Duncan, Mark Farnworth, Paul Warren, Nianhua Peng, Tien-Lin Lee, F. Louis, J. Piper, Regoutz Anna, Claire J. Carmalt,

- Ivan P. Parkin, Vin R. Dhanak, David O. Scanlon, Tim D. Veal, *Mater. Horiz.* (2020), <https://doi.org/10.1039/C9MH01014A>. Advance Article.
- [24] J.M. Langer, C. Delerue, M. Lannoo, *Phys. Rev. B* 38 (1988) 7723.
 - [25] C.J. Vesely, D.W. Langer, *Phys. Rev. B: Solid State* 4 (2) (1971) 451.
 - [26] P. King, T. Veal, A. Schleife, J. Zúñiga-Pérez, B. Martel, P. Jefferson, F. Fuchs, V. Muñoz-Sanjósé, F. Bechstedt, C. McConville, *Phys. Rev. B* 79 (2009) 205205.
 - [27] D.M. Detert, K. Tom, C. Battaglia, J. Denlinger, S.H.M. Lim, A. Javey, A. Anders, O.D. Dubon, K.M. Yu, W. Walukiewicz, *J. Appl. Phys.* 115 (2014) 233708.
 - [28] W. Shan, W. Walukiewicz, J.W. Ager III, E.E. Haller, J.F. Geisz, D.J. Friedman, J.M. Olson, S.R. Kurtz, *Phys. Rev. Lett.* 82 (1999) 1221.
 - [29] W. Walukiewicz, W. Shan, K.M. Yu, J.W. Ager III, E.E. Haller, I. Miotkowski, M.J. Seong, H. Alawadhi, A.K. Ramdas, *Phys. Rev. Lett.* 85 (2000) 1552.
 - [30] J. Wu, W. Shan, W. Walukiewicz, *Semicond. Sci. Technol.* 17 (8) (2002) 860–869.
 - [31] W. Walukiewicz, W. Shan, J. Wu, K.M. Yu, in: Irina Buyanova, Weimin Chen (Eds.), *Physics and Applications of Dilute Nitrides*, Taylor & Francis, New York, 2004, pp. 23–64 (Chapter 2).
 - [32] H. Fujiwara, M. Kondo, *Phys. Rev. B* 71 (2005), 075109.
 - [33] T. Pisarkiewicz, K. Zakrzewska, E. Leja, *Thin Solid Films* 174 (1989) 217.
 - [34] T. Pisarkiewicz, A. Kolodziej, Nonparabolicity of the conduction band structure in degenerate tin dioxide, *Phys. Status Solidi B* 158 (1990) K5.
 - [35] E. García-Hemme, K.M. Yu, P. Wahnnon, G. González-Díaz, W. Walukiewicz, *Appl. Phys. Lett.* 106 (2015) 182101.
 - [36] C.A. Francis, M. Jaquez, J.F. Sánchez-Royo, S.K.V. Farahani, C.F. McConville, J. Beeman, M. Ting, K.M. Yu, O.D. Dubón, W. Walukiewicz, *J. Appl. Phys.* 122 (2017) 185703.
 - [37] S.X. Li, E.E. Haller, K.M. Yu, W. Walukiewicz, J.W. Ager III, J. Wu, W. Shan, H. Lu, W.J. Schaff, *Appl. Phys. Lett.* 87 (2005) 161905.
 - [38] K.F. Berggren, B.E. Sernelius, *Phys. Rev. B* 24 (1981) 1971.
 - [39] D.M. Detert, K. Tom, C. Battaglia, J. Denlinger, S.H.M. Lim, A. Javey, A. Anders, O.D. Dubon, K.M. Yu, W. Walukiewicz, *J. Appl. Phys.* 115 (2014) 233708.